Available online at www.sciencedirect.com
SCIENCE DIRECT®
International Journal of Heat and Mass Transfer 47 (2004) 1917–1924
International Journal of HEAT and MASS TRANSFER
www.elsevier.com/locate/ijhmt

# Transient free convection in a square cavity filled with a porous medium

Nawaf H. Saeid [a,*], I. Pop [b]

[a] School of Mechanical Engineering, University of Science Malaysia, 14300 Nibong Tebal, Pulau Pinang, Malaysia
[b] Faculty of Mathematics, University of Cluj, R-3400 Cluj, CP 253, Romania

Received 25 June 2003; received in revised form 25 September 2003

**Abstract**

Transient free convection in a two-dimensional square cavity filled with a porous medium is numerically studied in this paper. The left vertical wall is suddenly heated to a constant temperature $T_h$, while the right wall is suddenly cooled to a constant temperature $T_c$ by equal amount relative to an initially uniform temperature distribution. Both the horizontal walls are adiabatic. The finite volume numerical method is used to solve the non-dimensional governing equations. The results are obtained for the initial transient state up to the steady state, and for Rayleigh number values of $10^2$–$10^4$. It is observed that the average Nusselt number showing an undershoot during the transient period and that the time required to reach the steady state is longer for low Rayleigh number and shorter for high Rayleigh number.


## 1. Introduction

Convective heat transfer in fluid-saturated porous media has received considerable attention over the last several decades. This interest was estimated due to many applications in, for example, packed sphere beds, high performance insulation for buildings, chemical catalytic reactors, grain storage and such geophysical problems as frost heave. Porous media are also of interest in relation to the underground spread of pollutants, solar power collectors, and to geothermal energy systems. Literature concerning convective flow in porous media is abundant. Representative studies in this area may be found in the recent books by Ingham and Pop [1], Nield and Bejan [2], Vafai [3], Pop and Ingham [4], and Bejan and Kraus [5].

Free convection in a cavity filled with a fluid-saturated porous medium is of prime importance in many technological applications. Examples are post-accident heat removal in nuclear reactors and geophysical problems associated with the underground storage of nuclear waste, among others. The problem of free convection in a rectangular porous cavity whose four walls are maintained at different temperatures or heat fluxes is one of the classical problems in porous media, which has been extensively studied. Much research work, both theoretical and experimental, has been done on this type of convective heat transfer processes. A good deal of references on this problem has been presented in the paper by Lauriat and Prasad [6], and in the recent paper by Baytas and Pop [7]. The model commonly used consists of a porous cavity with both the vertical walls maintained at constant temperatures, while the horizontal walls are adiabatic. The flow and heat transfer characteristics of the steady-state flow is generally studied for this type of cavity. However, a very little work has been done for the case of unsteady and transient flow situations.

The aim of this paper is to study numerically the problem of transient free convection in a square cavity filled with a porous medium when one of its vertical wall is suddenly heated and the other wall is suddenly cooled, while the horizontal walls are adiabatic. To our best knowledge, only Banu et al. [8] have presented a study of such a problem, but for a heat-generating porous cavity with all four walls maintained at a constant temperature.

* Corresponding author. Tel.: +60-4-593-7788; fax: +60-4-594-1025.
E-mail address: n_h_saied@yahoo.com (N.H. Saeid).

0017-9310/$ - see front matter 
doi:10.1016/j.ijheatmasstransfer.2003.10.014

**Nomenclature**

| | |
|---|---|
| $g$ | gravitational acceleration |
| $K$ | permeability of the porous medium |
| $L$ | cavity height/width |
| $Nu$ | local Nusselt number |
| $Ra$ | Rayleigh number for porous medium |
| $t$ | time |
| $T$ | fluid temperature |
| $u$, $v$ | velocity components along $x$- and $y$-axes, respectively |
| $U$, $V$ | non-dimensional velocity components along $X$- and $Y$-axes, respectively |
| $x$, $y$ | Cartesian coordinates |
| $X$, $Y$ | non-dimensional Cartesian coordinates |
| *Greek symbols* | |
| $\alpha$ | effective thermal diffusivity |
| $\beta$ | coefficient of thermal expansion |
| $\theta$ | non-dimensional temperature |
| $\nu$ | kinematic viscosity |
| $\sigma$ | ratio of composite material heat capacity to convective fluid heat capacity |
| $\tau$ | non-dimensional time |
| $\psi$ | stream function |
| $\Psi$ | non-dimensional stream function |

## 2. Basic equations

A schematic diagram of a two-dimensional square cavity is shown in Fig. 1. It is assumed that the left vertical wall of the cavity is suddenly heated to the constant temperature $T_h$ and the right vertical wall is suddenly cooled to the constant temperature $T_c$, where $T_h > T_c$, by equal amount relative to an initially uniform temperature distribution, while the horizontal walls are adiabatic.

In the porous medium, Darcy's law is assumed to hold, and the fluid is assumed to be a normal Boussinesq fluid. The viscous drag and inertia terms in the governing equations are neglected, which are valid assumptions for low Darcy and particle Reynolds numbers. With these assumptions, the continuity, Darcy and energy equations for unsteady, two-dimensional flow in an isotropic and homogeneous porous medium are

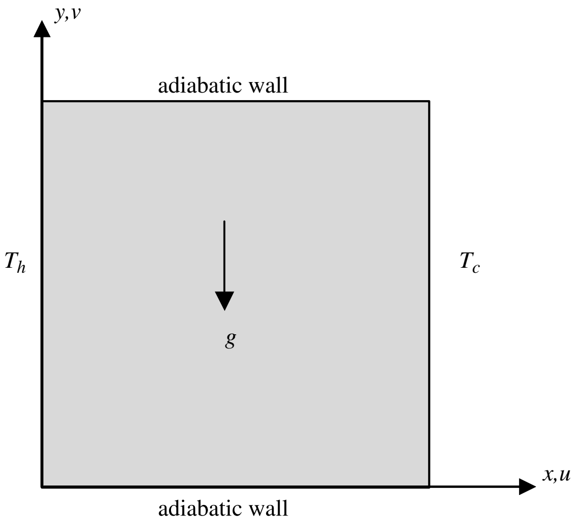


Fig. 1. Schematic diagram of the physical model and coordinate system.

$$\frac{\partial u}{\partial x} + \frac{\partial v}{\partial y} = 0 \tag{1}$$

$$\frac{\partial u}{\partial y} - \frac{\partial v}{\partial x} = -\frac{g\beta K}{\nu}\frac{\partial T}{\partial x} \tag{2}$$

$$\sigma\frac{\partial T}{\partial t} + u\frac{\partial T}{\partial x} + v\frac{\partial T}{\partial y} = \alpha\left(\frac{\partial^2 T}{\partial x^2} + \frac{\partial^2 T}{\partial y^2}\right) \tag{3}$$

where $u$, $v$ are the velocity components along $x$- and $y$-axes, $T$ is the fluid temperature and the physical meaning of the other quantities are mentioned in the Nomenclature. The above equations are subjected to the following initial and boundary conditions:

$$u(x,y,0) = v(x,y,0) = 0, \quad T(x,y,0) = T_0 \tag{4a}$$

$$u(0,y,t) = v(0,y,t) = 0, \quad T(0,y,t) = T_h \tag{4b}$$

$$u(L,y,t) = v(L,y,t) = 0, \quad T(L,y,t) = T_c \tag{4c}$$

$$u(x,0,t) = v(x,0,t) = 0, \quad \partial T(x,0,t)/\partial y = 0 \tag{4d}$$

$$u(x,L,t) = v(x,L,t) = 0, \quad \partial T(x,L,t)/\partial y = 0 \tag{4e}$$

where $T_0 = (T_h + T_c)/2$. Eqs. (1)–(3) can be written in terms of the stream function $\psi$ defined as $u = \partial\psi/\partial y$ and $v = -\partial\psi/\partial x$ together with the following non-dimensional variables:

$$X = \frac{x}{L}, \quad Y = \frac{y}{L}, \quad \tau = \frac{\alpha t}{\sigma L^2}, \quad \theta = \frac{T - T_0}{T_h - T_c},$$
$$\Psi = \frac{\psi}{\alpha} \tag{5}$$

The non-dimensional forms of the governing Eqs. (1)–(3) are:

$$\frac{\partial^2\Psi}{\partial X^2}+\frac{\partial^2\Psi}{\partial Y^2}=-Ra\frac{\partial\theta}{\partial X} \tag{6}$$

$$\frac{\partial\theta}{\partial\tau}+\frac{\partial\Psi}{\partial Y}\frac{\partial\theta}{\partial X}-\frac{\partial\Psi}{\partial X}\frac{\partial\theta}{\partial Y}=\frac{\partial^2\theta}{\partial X^2}+\frac{\partial^2\theta}{\partial Y^2} \tag{7}$$

where $Ra$ is the Rayleigh number defined as: $Ra = g\beta K\Delta TL/\nu\alpha$, and the initial and boundary conditions (4) become

$$\Psi(X,Y,0)=0,\quad \theta(x,y,0)=0 \tag{8a}$$

$$\Psi(0,Y,\tau)=0,\quad \theta(0,Y,\tau)=0.5 \tag{8b}$$

$$\Psi(1,Y,\tau)=0,\quad \theta(1,Y,\tau)=-0.5 \tag{8c}$$

$$\Psi(X,0,\tau)=0,\quad \partial\theta(X,0,\tau)/\partial Y=0 \tag{8d}$$

$$\Psi(X,1,\tau)=0,\quad \partial\theta(X,1,\tau)/\partial Y=0 \tag{8e}$$

The physical quantities of interest in this problem are the local Nusselt number along the hot wall, defined by

$$Nu=\left(-\frac{\partial\theta}{\partial X}\right)_{X=0} \tag{9}$$

and also the average Nusselt number, which is defined as

$$\overline{Nu}=\int_0^1 Nu\,\mathrm{d}Y \tag{10}$$

## 3. Numerical method

Eqs. (6) and (7) subject to the boundary conditions (8) are integrated over a control volume using the fully implicit scheme which is unconditionally stable. The power-law scheme is used for the convection–diffusion formulation as describe by Patankar [9]. The solution domain, therefore, consists of grid points at which the discretization equations are applied. In this domain $X$ an $Y$, by definition varies from 0 to 1, non-uniform grid has been selected in both $X$ and $Y$ directions such that the grid points clustered near the walls. The grid size and geometry were tested, and it was found that the following size and geometry give the best results comparing with the results in the literature for the steady-state flow: the grid size is (41×41) and the grid geometry is symmetrical about the centerlines. The grid points on the left-hand side from the vertical centerline are defined as

$$X(i)=\frac{1}{2}\left(\frac{i-1}{N_{\mathrm{cl}}-1}\right)^{1.2},\quad i=1,2,\ldots,N_{\mathrm{cl}} \tag{11a}$$

where $N_{\mathrm{cl}}$ is the centerline grid point index ($N_{\mathrm{cl}}=21$) and $X(N_{\mathrm{cl}})=1/2$. The grid spacing can be calculated from

$$\Delta X(i)=X(i+1)-X(i),\quad i=1,2,\ldots,(N_{\mathrm{cl}}-1) \tag{11b}$$

The grid spacing in the right hand side from the centerline is calculated from the similarity

$$\Delta X(N-i)=\Delta X(i),\quad i=1,2,\ldots,(N_{\mathrm{cl}}-1) \tag{11c}$$

Finally, the grid points on the right hand side from the centerline are calculated as

$$X(i+1)=X(i)+\Delta X(i),\quad i=N_{\mathrm{cl}},N_{\mathrm{cl}}+1,\ldots,(N-1) \tag{11d}$$

The same method is used to define and stretch the grid in the $Y$ direction. The time step is chosen to be uniform $\Delta\tau=10^{-4}$, which has been used also by Baytas and Pop [7]. The resulting algebraic equations were solved by line-by-line iteration using Tri-Diagonal Matrix Algorithm. The iteration process is terminated under the following condition

$$\sum_{i,j}|\phi^n_{i,j}-\phi^{n-1}_{i,j}|\Big/\sum_{i,j}|\phi^n_{i,j}|\leqslant 10^{-5} \tag{12}$$

where $\phi$ stands for $\theta$ and $\Psi$; $n$ denotes the iteration step.

## 4. Results and discussion

The streamlines and isotherms at different time steps ranging from $\tau=0.0025$ to $\tau=0.08$ are shown in Fig. 2 for $Ra=1000$. It can be seen that early in the transient, the isotherms are nearly parallel indicating conduction heat transfer and the fluid is rising up near the hot left wall and is fallen downward near the cooled right wall, respectively. A recirculation flow region of small intensity sites close to the upper part of the hot wall or to the lower part of the cooled wall and spin the fluid towards the center of the enclosure (Fig. 2a). Shortly after that, the fluid travels across the upper (or lower) half of the enclosure (Fig. 2b). The streamlines indicate an elongation of the recirculating region of the flow along with a transition to the middle of the enclosure (Fig. 2b). With increasing of time ($\tau=0.01$), the majority of fluid is rising up or falling down near the hot wall and near the cooled wall, respectively (Fig. 2c) and the local Nusselt number is continuously decreasing near the upper part of the hot wall (Fig. 3b). Further, after a short time ($\tau=0.02$), the flow has been extended throughout the cavity and convection has became more important (Fig. 2d). For $\tau>0.04$ the flow is then going to attain the steady-state regime (Fig. 2e), which happens for $\tau=0.08$ (Fig. 2f). The streamlines and the isotherms at $\tau=0.08$ presented in Fig. 2f are almost identical to those given by Baytas and Pop [7], and Baytas [10]. The development of the velocity and thermal boundary layers on the vertical walls of the cavity can be clearly observed from these figures, which continuously grow to the steady-state thermal boundary layers flow. The development of the velocity and thermal boundary layers for $Ra=10^2$ and $10^4$ are similar to

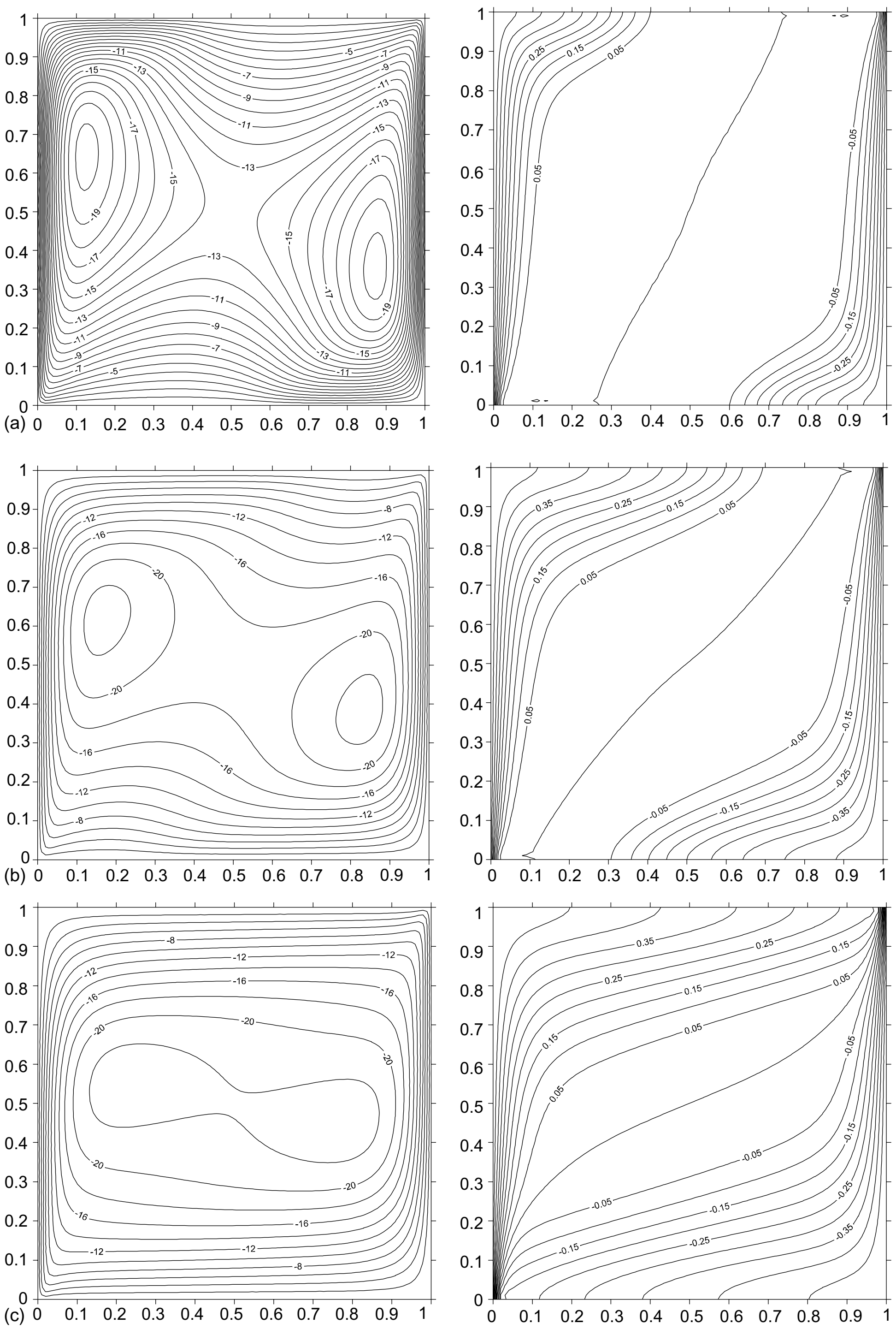


Fig. 2. Stream lines (left) and isotherms (right) for $Ra = 1000$; (a) and $\tau = 0.0025$, (b) and $\tau = 0.005$, (c) and $\tau = 0.01$, (d) and $\tau = 0.02$, (e) and $\tau = 0.04$ and (f) and $\tau = 0.08$.

those shown in Fig. 2. The difference is that for low Rayleigh number condition the convection currents will be weaker which leads to the grow of the boundary layer will be slower than for high Rayleigh number condition. The stream lines and the isotherms for $Ra = 10^2$ and $10^4$ are not shown for brevity.

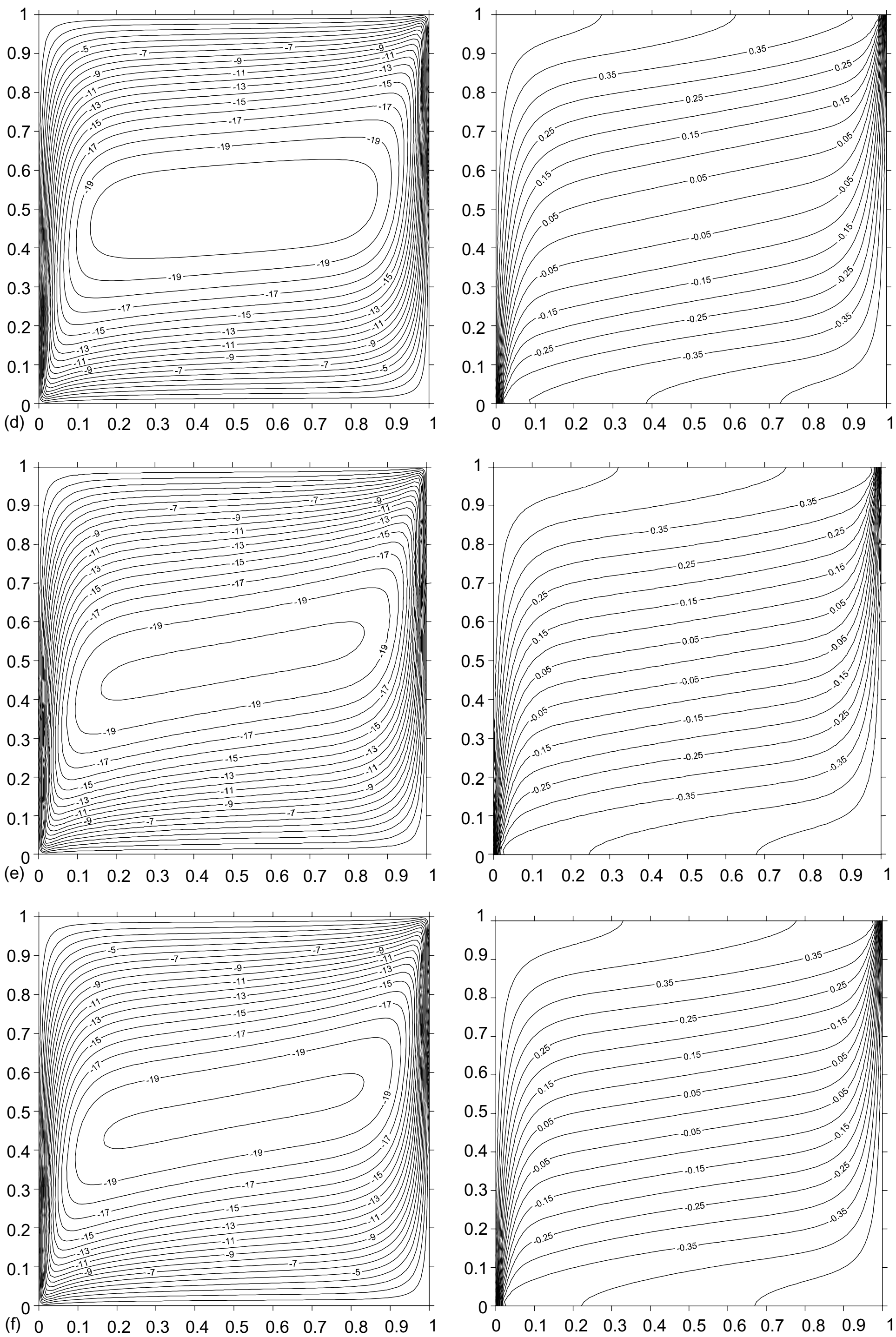


Fig. 2 (*continued*)

The variation of the transient local Nusselt number with time $\tau$ along the hot wall of the cavity at different positions $Y$ is presented in Fig. 3 for $Ra = 10^2$–$10^4$. It is seen that immediately after the process of impulsively heating starts the value of the local Nusselt number goes to infinity (is singular) and this is characteristic to any impulsively started heating system. Then, at small positions ($Y < 0.5$), the local Nusselt number decreases for a short time followed by a constant value and then increase to reach the steady state value. Fig. 3c shows that this phenomenon will happen for the upper half also ($Y \geqslant 0.5$) for $Ra = 10^4$. However, for $Y \geqslant 0.5$ and $Ra = 10^2$ and $10^3$ the local Nusselt number decreases continuously with increasing the time until it reaches its steady-state value. This variation of the transient local Nusselt number is reflected on the average Nusselt number which is defined in Eq. (10). Fig. 4 shows the variation of the average Nusselt number with the non-dimensional time for different Rayleigh numbers. The average Nusselt number showing an undershoot during the transient period followed by a constant steady state value for all $Ra = 10^2$–$10^4$. It is also observed that the time required to reach the steady state ($Nu$ becomes constant) is longer for low Rayleigh number and shorter for high Rayleigh number as shown in Figs. 3 and 4.

Further, values of the average Nusselt number along the hot wall of the cavity at the steady-state flow for $Ra = 10^2$–$10^4$ are given in Table 1. It is seen again that

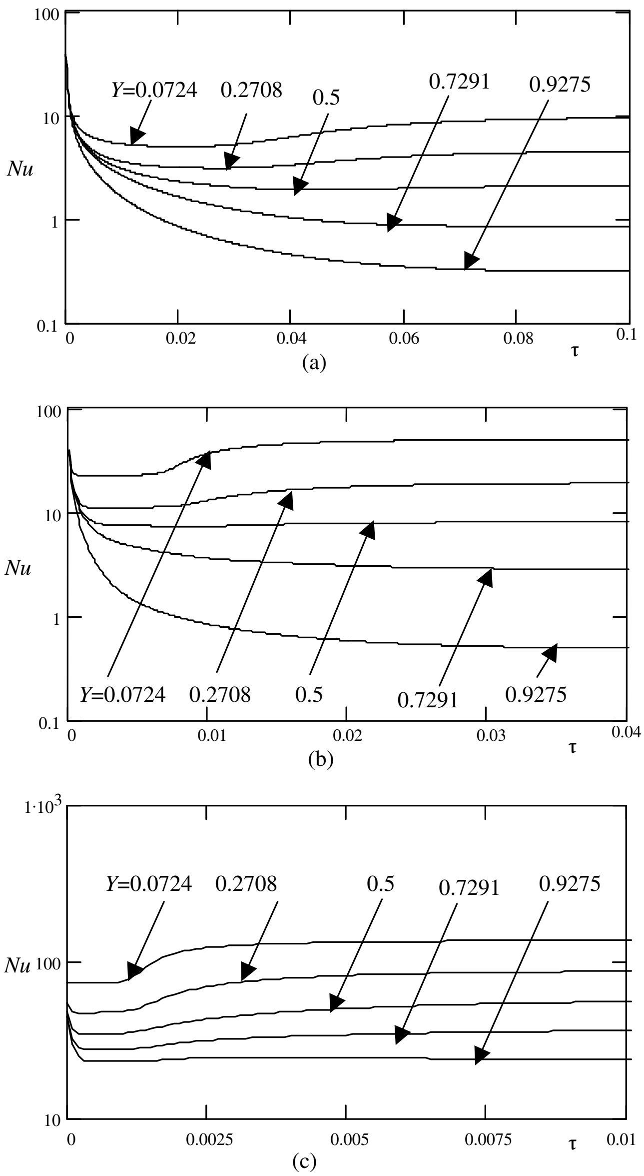


Fig. 3. Variation of the transient local Nusselt number with $\tau$ at different Rayleigh number: (a) $Ra = 100$, (b) $Ra = 1000$ and (c) $Ra = 10000$.

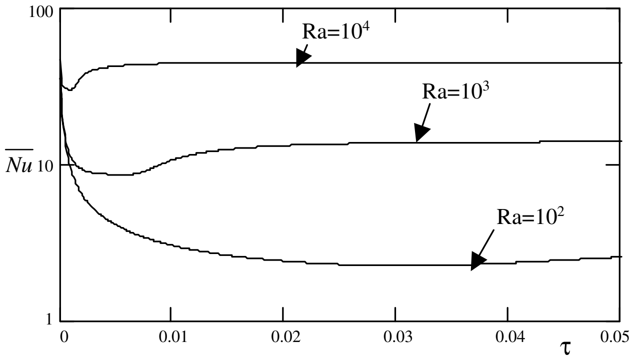


Fig. 4. Variation of the transient average Nusselt number with $\tau$ at different Rayleigh number.

Table 1
Comparison of $\overline{Nu}$ at steady state with some previous numerical results

| Author | $\overline{Nu}$ | | |
|---|---|---|---|
| | $Ra = 100$ | $Ra = 1000$ | $Ra = 10,000$ |
| Walker and Homsy [11] | 3.097 | 12.960 | 51.000 |
| Bejan [12] | 4.200 | 15.800 | 50.800 |
| Gross et al. [13] | 3.141 | 13.448 | 42.583 |
| Manole and Lage [14] | 3.118 | 13.637 | 48.117 |
| Baytas [10] | 3.160 | 14.060 | 48.330 |
| Present results | 3.002 | 13.726 | 43.953 |

the present values of $\overline{Nu}$ are in very good agreement with that obtained by different authors, such as Walker and Homsy [11], Bejan [12], Gross et al. [13], and Manole and Lage [14]. Therefore, these results provide great confidence to the accuracy of the present numerical model.

It is important to recall that the above results were obtained using the thermal equilibrium between the solid and fluid phases in the porous media assuming low Reynolds number and low porosity. The effect of the non-equilibrium is usually considered for higher fluid velocity as well as higher porosity which need further investigation as extension to the present research.

## 5. Conclusions

The transient free convection in a two-dimensional square cavity filled with a porous medium is considered in this paper. The flow is driven by considering the case when one of the cavity vertical walls is suddenly heated and the other vertical wall is suddenly cooled, while the horizontal walls are adiabatic. The non-dimensional forms of the continuity, Darcy and energy equations are solved numerically. The power-law scheme is used for the convection–diffusion formulation in the non-uniform grid in both horizontal and vertical directions. It is observed during the transient period the average Nusselt number showing an undershoot followed by a constant steady state value for all $Ra = 10^2$–$10^4$ and at the steady state the flow and heat transfer characteristics are similar to those from the open literature. It is also observed that the time required to reach the steady state is longer for low Rayleigh number and shorter for high Rayleigh number.

## Acknowledgements

The authors wish to thank the anonymous referees. Their comments led to substantial improvements of the first manuscript.

## References

[1] D.B. Ingham, I. Pop (Eds.), Transport Phenomena in Porous Media, Pergamon, Oxford, vol. II, 1998, 2002.
[2] D.A. Nield, A. Bejan, Convection in Porous Media, second ed., Springer, New York, 1999.
[3] K. Vafai (Ed.), Handbook of Porous Media, Marcel Dekker, New York, 2000.
[4] I. Pop, D.B. Ingham, Convective Heat Transfer: Mathematical and Computational Modelling of Viscous Fluids and Porous Media, Pergamon, Oxford, 2001.
[5] A. Bejan, A.D. Kraus (Eds.), Heat Transfer Handbook, Wiley, New York, 2003.
[6] G. Lauriat, V. Prasad, Natural convection in a vertical porous cavity: A numerical study for Brinkman-extended

Darcy formulation, J. Heat Transfer 109 (1987) 688–696.

[7] A.C. Baytas, I. Pop, Free convection in a square porous cavity using a thermal nonequilibrium model, Int. J. Therm. Sci. 41 (2002) 861–870.

[8] N. Banu, D.A. Rees, I. Pop, Steady and unsteady free convection in porous cavities with internal heat generation, in: Heat Transfer 1998, Proceedings of 11th IHTC, vol. 4, Kyongju, Korea, 1998, pp. 375–380.

[9] S.V. Patankar, Numerical Heat Transfer and Fluid Flow, Hemisphere Publishing Corporation, Washington, 1980.

[10] A.C. Baytas, Entropy generation for natural convection in an inclined porous cavity, Int. J. Heat Mass Transfer 43 (2000) 2089–2099.

[11] K.L. Walker, G.M. Homsy, Convection in a porous cavity, J. Fluid Mech. 87 (1978) 449–474.

[12] A. Bejan, On the boundary layer regime in a vertical enclosure filled with a porous medium, Lett. Heat Mass Transfer 6 (1979) 93–102.

[13] R.J. Gross, M.R. Bear, C.E. Hickox, The application of flux-corrected transport (FCT) to high Rayleigh number natural convection in a porous medium, in: Proceedings of 8th International Heat Transfer Conference, San Francisco, CA, 1986.

[14] D.M. Manole, J.L. Lage, Numerical benchmark results for natural convection in a porous medium cavity, in: HTD-vol. 216, Heat and Mass Transfer in Porous Media, ASME Conference, 1992, pp. 55–60.